

Report No. NA-67-1  
(DS-67-23)

45

FINAL REPORT

Project No. 540-008-01X

AN ANALYSIS OF THE HELICOPTER HEIGHT VELOCITY DIAGRAM  
INCLUDING A PRACTICAL METHOD FOR ITS DETERMINATION



D D C  
R R R R R R R R  
MAY 28 1968  
R R R R R R R R  
B R B R B R B R B

FEBRUARY 1968

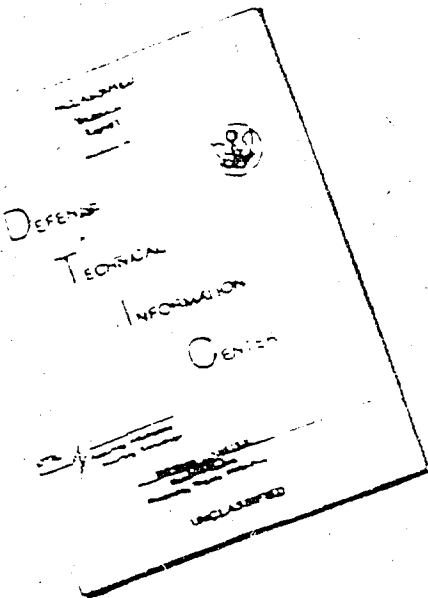
1968 EDITION OF THIS DOCUMENT IS UNCLASSIFIED  
for public release under the Freedom of Information Act  
Distribution is unlimited

DEPARTMENT OF TRANSPORTATION  
Federal Aviation Administration  
National Aviation Facilities Experimental Center  
Atlantic City, New Jersey 08405

Reproduced by the  
**CLEARINGHOUSE**  
for Federal Scientific & Technical  
Information Springfield Va 22151

36

# DISCLAIMER NOTICE



THIS DOCUMENT IS BEST  
QUALITY AVAILABLE. THE COPY  
FURNISHED TO DTIC CONTAINED  
A SIGNIFICANT NUMBER OF  
PAGES WHICH DO NOT  
REPRODUCE LEGIBLY.

THIS DOCUMENT CONTAINED  
BLANK PAGES THAT HAVE  
BEEN DELETED

REPRODUCED FROM  
BEST AVAILABLE COPY

This Document Contains  
Missing Page/s That Are  
Unavailable In The  
Original Document

FINAL REPORT

AN ANALYSIS OF THE HELICOPTER WRIGHT VELOCITY DIAGRAM  
INCLUDING A PRACTICAL METHOD FOR ITS DETERMINATION

Project No. 340-006-01X  
Report No. NA-67-1  
(DS-67-23)

Prepared by:

WILLIAM J. HANLEY  
GILBERT DEVORE

for

AIRCRAFT DEVELOPMENT SERVICE

FEBRUARY 1968

Distribution of this document is unlimited. This document does not necessarily reflect Federal Aviation Administration policy in all respects and it does not, in itself, constitute a standard, specification, or regulation.

Department of Transportation  
Federal Aviation Administration  
National Aviation Facilities Experimental Center  
Atlantic City, N. J. 08405

## ABSTRACT

A composite summary analysis was made of the height-velocity (H-V) diagram test data obtained from the flight testing of three single engine, single rotor helicopters of varying design characteristics and basic parameters. The purpose of this analysis was to ascertain if a practical method for the determination of the H-V diagram could be evolved, as well as a means to determine the effects of aircraft weight and altitude on the H-V diagram. Analysis disclosed that H-V diagrams can be developed for any conventional single rotor helicopter by the flight test determination of a single maximum performance critical speed ( $V_{cr}$ ) point in conjunction with the use of a non-dimensional curve and the solution of specific key point ratios which are set forth in the report. An evaluation of the H-V diagram key point relationships is presented followed by a discussion of the observed factors affecting autorotative landing following power failure. A suggested step by step procedure for flight manual type H-V diagrams is also presented.

## TABLE OF CONTENTS

	Page
<b>ABSTRACT</b>	1-1
<b>INTRODUCTION</b>	1
<b>Purpose</b>	1
<b>Background</b>	1
<b>DISCUSSION</b>	2
<b>Test Aircraft</b>	2
<b>Test Instrumentation</b>	4
<b>Test Procedures</b>	4
<b>Basic Test Methodology</b>	4
<b>Maximum Performance</b>	4
<b>Test Weights and Altitudes</b>	4
<b>Flight Entry Condition</b>	5
<b>Touchdown Speeds</b>	5
<b>SUMMARY OF RESULTS</b>	6
<b>Scope</b>	6
<b>Height-Velocity Diagrams</b>	6
<b>General</b>	6
<b>Generalized Height-Velocity Curve</b>	6
<b>Evaluation of Key Point Relationships</b>	10
<b>Critical Speed Versus Weight</b>	10
<b>Critical Speed Versus Altitude</b>	12
<b>The Critical Height</b>	12
<b>Critical Speed Squared Versus High Hover Height</b>	13
<b>Low Hover Height Versus Weight and Altitude</b>	13
<b>Factors Affecting the Autorotative Landing Following Power Failure</b>	15
<b>Motor Inertia and Rotor Speed</b>	15
<b>Blade Stall Considerations</b>	17
<b>The Maneuver - Cyclic and Collective Flare</b>	17
<b>Method of Converting Test Program H-V Diagrams to Flight</b>	21
<b>Manual Type H-V Diagrams</b>	21
<b>Procedures for Obtaining Flight Manual Type H-V Diagrams for Range of Weights and Altitudes</b>	22
<b>CONCLUSIONS</b>	24
<b>RECOMMENDATIONS</b>	25
<b>REFERENCES</b>	26
<b>APPENDIX I Glossary of Terms (2 pages)</b>	I-1

## LIST OF ILLUSTRATIONS

Figure		Page
1	Test Aircraft	3
2	Typical H-V Diagrams	7
3	Method of Converting Typical H-V Diagram Into Calculated Key Point Ratios	8
4	Composite Non-Dimensional Curve	9
5	$C_l$ Versus Disk Area	11
6	High Hover Height ( $h_{min}$ ) Versus Square of Critical Velocity ( $V_{c,r}^2$ )	14
7	Average Rotor Speed Decay Trends from High Hover Entry Points	16
8	Comparison of Time History Data For High Hover Points - Three Test Helicopters	18
9	Comparison of Time History Data For Critical Speed Area ( $V_{cr}, h_{cr}$ ) - Three Test Helicopters	19
10	Comparison of Time History Data For Low Hover Points - Three Test Helicopters	20

LIST OF TABLES

Table		Page
I	Test Aircraft Characteristics	2
II	Test Weights and Elevations	5

## INTRODUCTION

### Purpose

The purpose of this project was to determine the effects of aircraft weight and altitude on the basic Height Velocity (H-V) diagrams of three helicopters, and to ascertain if a practical method could be developed for determining the family of curves by analysis rather than by extensive flight testing.

### Background

A long-range flight test program was initiated by the Aircraft Development Service, Federal Aviation Administration (FAA), to determine the effects of altitude and weight on the helicopter H-V diagram through actual flight tests. The program was established in response to a need to obtain a practical approach for the determination of the effects of altitude and weight on the helicopter H-V diagram, and for safe autorotational landing criteria in general. In this study only the low speed portion of the H-V diagram was considered. It was felt that the high speed portion involved other considerations that were not pertinent to this analysis and the high speed portion was considered to be not as important as the low speed portion. Within the framework of this program, the testing of three different helicopters possessing widely varying parameters was accomplished in individual but objectively related projects. The results of these tests were published in References 1, 2, and 3.

The H-V envelope for each of the helicopters tested was found to vary as a function of gross weight and density altitude. The similarity of the effects of weight and altitude on the H-V diagrams of the helicopters tested, and the accumulation of helicopter autorotational landing characteristics data warranted an attempt to correlate all the facts. The results of this effort are presented in this report which:

1. Evaluates and summarizes the significant findings of three helicopter H-V flight test projects as individually reported in the FAA Technical Reports, Nos. ADS-1, ADS-46, and ADS-84.
2. Presents empirical factors and a method for the determination of the H-V diagram of conventional single rotor helicopters.
3. Discusses observations of the factors which influence the determination of the critical velocity of the H-V diagram and autorotational landing characteristics in general.

## DISCUSSION

### Test Aircraft

The three helicopters tested under the long-range program were all single engine, single rotor helicopters as shown in Fig. 1. Helicopter No. 1 was a lightweight model with relatively low disk loading and moderate rotor inertia. On the other hand, Helicopter No. 2 was also a lightweight model but with a comparatively high disk loading and a low rotor inertia. Helicopter No. 3 was a large, heavyweight helicopter with high disk loading and a comparatively high rotor inertia. Tabulated in Table I are some of the basic parameters which further define the three helicopters and which were involved in the analytical study that was the basis of this report. It was considered that a representative cross section of helicopters was chosen with respect to design considerations as they might influence the test results. Of the three helicopters tested, only Helicopter No. 1 had an altitude rated powerplant system while Helicopters Nos. 2 and 3 essentially had sea level rated systems; consequently, tests at high airport elevations with the latter two helicopters could not be conducted at all the desired test weights because of the power-on performance characteristics. More detailed specifications on the test helicopters are presented in References 1, 2, and 3 which are the basic references of this report.

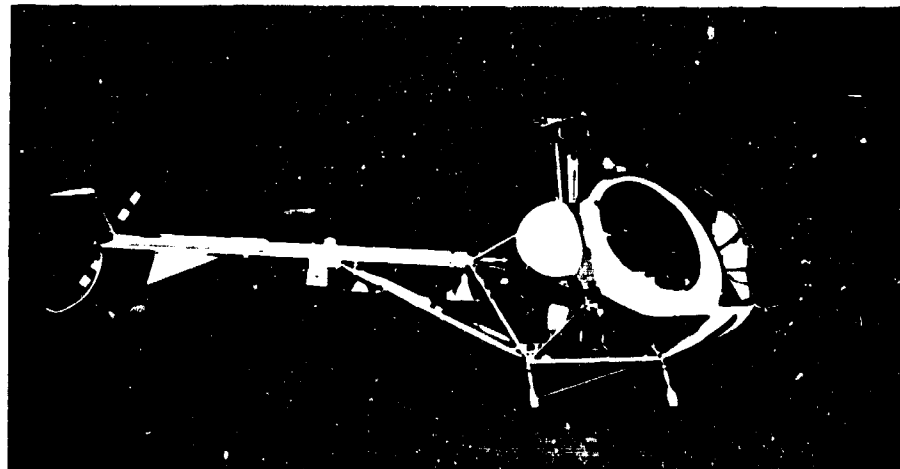
TABLE I  
TEST AIRCRAFT CHARACTERISTICS

	<u>Unit</u>	Helicopter No. 1	Helicopter No. 2	Helicopter No. 3
Max. Cert. Gross Weight	lbs	2850	1670	13,000
hp/rpm @ S.L. continuous	hp/rpm	220/3200	160/2700	1275/2500
Disk Loading W/A	lb/ft <sup>2</sup>	2.63	3.32	5.28
Rotor Solidity Ratio, $\sigma$		.0314	.0424	.059
Rotor Inertia, $I_R$	slug ft <sup>2</sup>	710	140	5800
No. of Rotor Blades		2	3	4
Landing Gear Config.		Skid	Skid	Wheel
Rotor Config.		Teetering	Articulated	Articulated
* Equiv. Flat Plate Area	ft <sup>2</sup>	18	14.5	36.5
Rotor Disk Area, A	ft <sup>2</sup>	1083	503	2460
Rotor Tip Speed, $R\Omega$	ft/sec	690	640	700

\*Frontal



HELICOPTER NO. 1



HELICOPTER NO. 2



HELICOPTER NO. 3

FIG. 1 TEST AIRCRAFT

### Test Instrumentation

Airborne and ground instrumentation was utilized to record helicopter performance, aircraft space position and meteorological information. In general, the same parameters were measured with identical or similar instrumentation for all three flight test projects.

### Test Procedures

#### 1. Basic Test Methodology

Early in the planning stages, certain basic ground rules were established as mandatory and applicable throughout all the project tests. Essentially, these guidelines were as follows:

##### a. Maximum Performance

The H-V diagrams developed had to be representative of a maximum performance effort; that is, it was necessary to extract the maximum capabilities from the helicopter during each and every test point throughout the entire program. This was necessary since there were no known parameters available by which a fixed degree of conservatism in obtaining these test points could be determined or measured. Extraction of the maximum performance capability of the aircraft is dependent upon the skill of the pilot. For this reason, professional engineering test pilots, thoroughly familiar with the helicopter each flew, and well skilled in the mechanics of determining H-V diagrams, were employed for the piloting function.

##### b. Test Weights and Elevations

The weights and elevations selected for each of the helicopters tested were chosen with sufficient spread to clearly indicate the effects of these variables on the H-V diagram. The test sites selected provided a broad range of density altitudes and the incremental weight changes averaged approximately 8% of maximum certificated gross weight. Table II lists the test site elevations and helicopter weights used in the program.

		TABLE II		
		TEST WEIGHTS AND ALTITUDE		
ALTITUDE (ft) MILL	Aircraft Test Weight (lbs)			
	Helicopter No. 1 2913 3030 3030	Helicopter No. 2 1420 1600	Helicopter No. 3 2100 10,100 11,100	
117				X X X
332	X X X	X X		
4110	X X X	X X		X X X
6263				X X
7120	X X X	X		
9870	X X			

X Indication with elevation/weight combination for flight tests.

Note: Density Altitudes at time of tests were generally higher than field elevations.

#### c. Flight Entry Conditions

All of the simulated power failure landing maneuvers had to be executed from a trim, steady state, level flight entry condition in order to obtain repeatability and accuracy. The use of an accelerated climbout technique along the lower boundary was deemed to include too many variables to provide the accuracy required for the basic determination. Admittedly, the accelerated climbout technique would have provided a more realistic approach, but in addition to the requirements for repeatability, safety as well as the economics of the program also had to be considered. It was, therefore, decided that the level flight technique was the best compromise.

For test points along the upper boundary, collective pitch reduction was applied with a one-second delay after simulated power failure as well as with no-delay. For all test points initiated along the lower boundary, collective pitch reduction, when applied, was immediate.

#### d. Touchdown Speeds

There were no limitations placed upon the pilots' ~~discrepancy~~ respect to touchdown speeds. They were allowed to contact the runway at whatever forward velocity was required in order to fulfill the requirements of extracting the maximum capability of the aircraft for every landing.

## SUMMARY OF RESULTS

### Results

An analysis of the test data of the total program was undertaken to determine if sufficient data existed to permit the formulation of an empirical and/or theoretical method of predicting the size and shape of the H-V diagram for conventional single rotor helicopters.

### Height-Velocity Diagrams

#### 1. General

The height-velocity diagrams developed for each helicopter exhibited remarkable similarity in shape to each other. Each helicopter tested produced a family of H-V diagrams which reflected the effects of weight and altitude, and each of these families was similar to the families of the other helicopters not only in shape but in the relationship of all the key points.

This similarity existed for the conditions of both no-delay and one-second delay in pitch reduction following simulated power failure. A typical example of H-V diagrams developed in this program is shown in Figure 2, on which the basic key points are designated. The fact that a family of curves existed that were so similar gave rise to the concept of a nondimensional curve that could be utilized to facilitate computation of H-V diagrams.

#### 2. Generalized Height-Velocity Curve

Each of the helicopters tested produced a family of diagrams which were related as functions of weight and altitude; therefore, the family of diagrams for each helicopter could be presented in the form of one nondimensional H-V curve. This procedure was first suggested in Reference 4, and was more recently accomplished in Reference 5, utilizing the data developed in one of the tests of this program. The H-V families of all three helicopters have been further combined in this summary analysis to form one composite nondimensional H-V curve. The composite nondimensional H-V curve was generated by computing the key point ratios  $V_n/V_{cr}$ ,  $h_1$ , and  $h_2$  as shown on Figure 3. All of the H-V diagrams developed in this program were nondimensionalized in accordance with the procedure shown on Figure 3 and the resulting nondimensional points were plotted on Figure 4.

A mean nondimensional H-V curve was then constructed through the composite data. A table has been prepared which presents the coordinates of this mean H-V curve. It is thus possible to construct an H-V diagram for any weight (minimum operating to maximum gross) and altitude (8,000 ft maximum) when one of the key points,  $h_{min}$  or  $V_{cr}$ , is known by reversing the above procedure. Utilizing the mean values of the chart on Figure 4, the ratios can be solved for values of  $h_n$  and  $V_n$ .

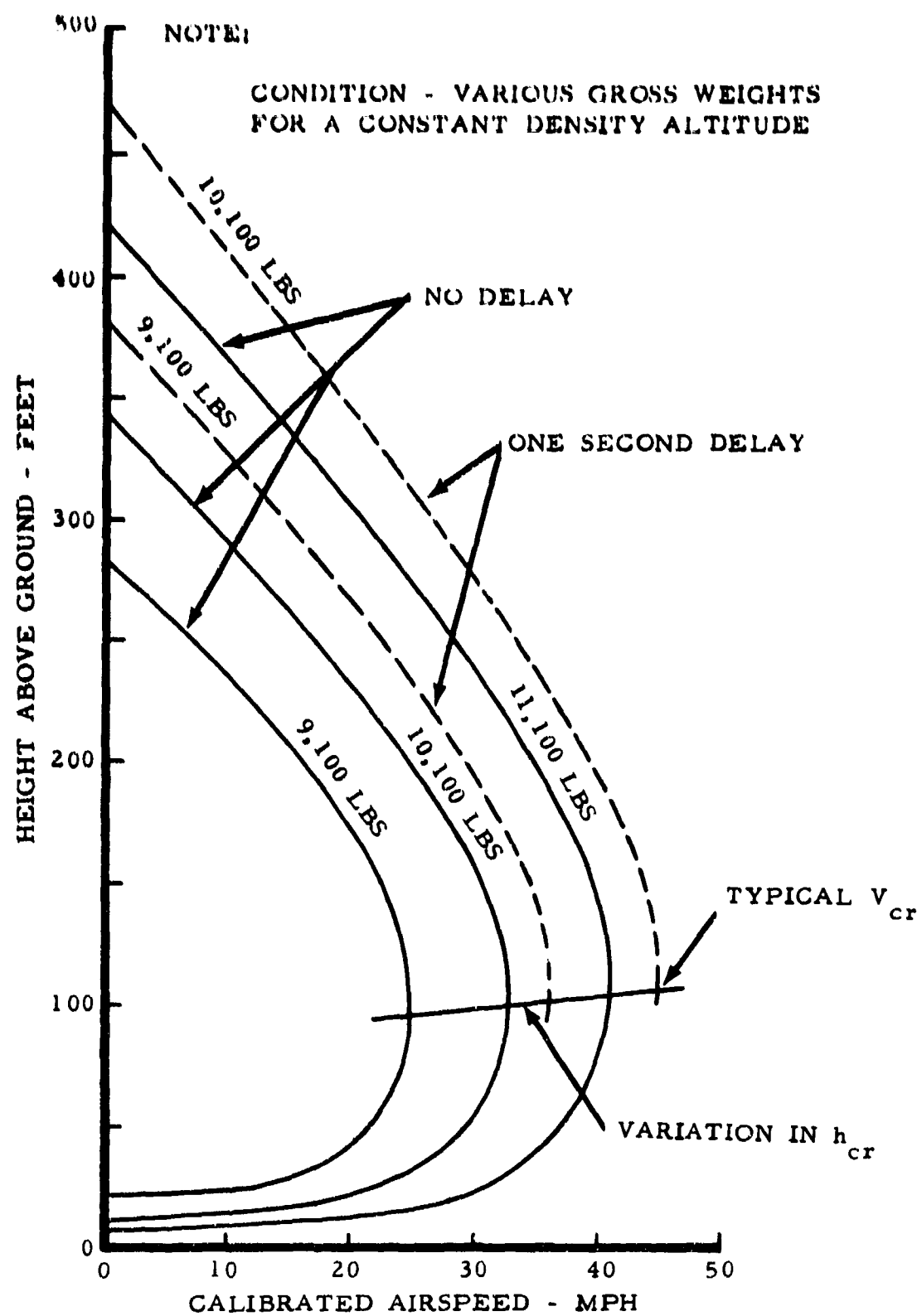
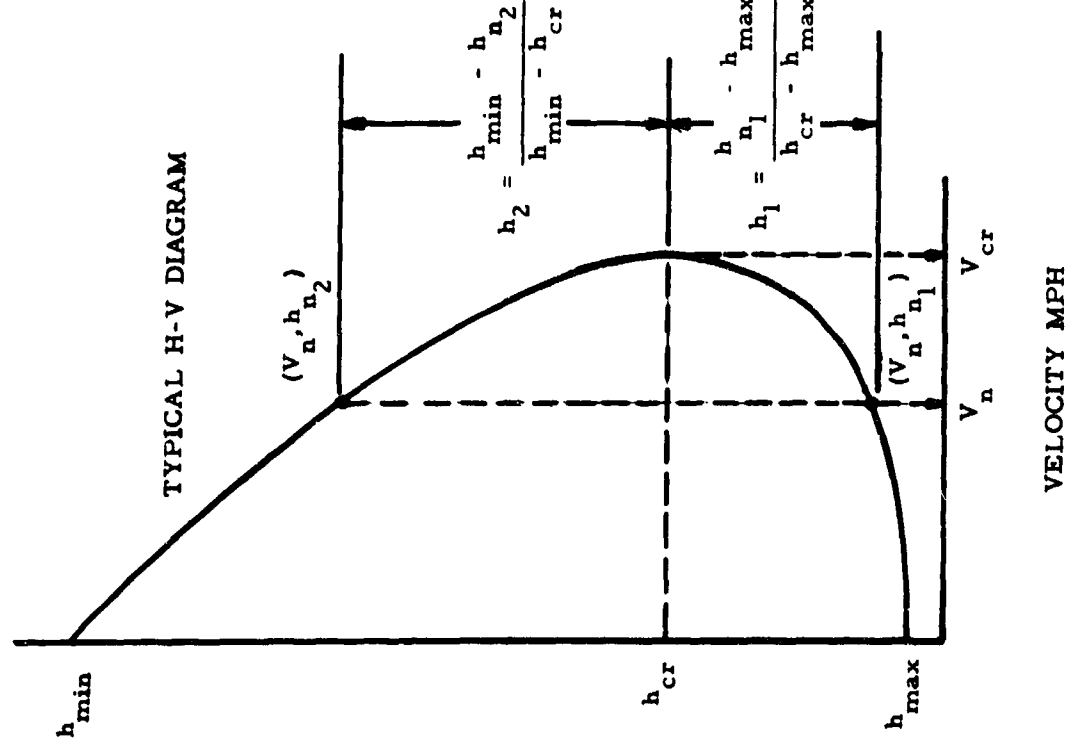


FIG. 2 TYPICAL H-V DIAGRAMS

TYPICAL H-V DIAGRAM



NON-DIMENSIONALIZING PROCEDURE

1. NON-DIMENSIONAL VELOCITY  
AT A SELECTED VELOCITY VALUE  $V_n$ ,  
DIVIDE BY VALUE  $V_{cr}$  TO OBTAIN NON-  
DIMENSIONAL VELOCITY

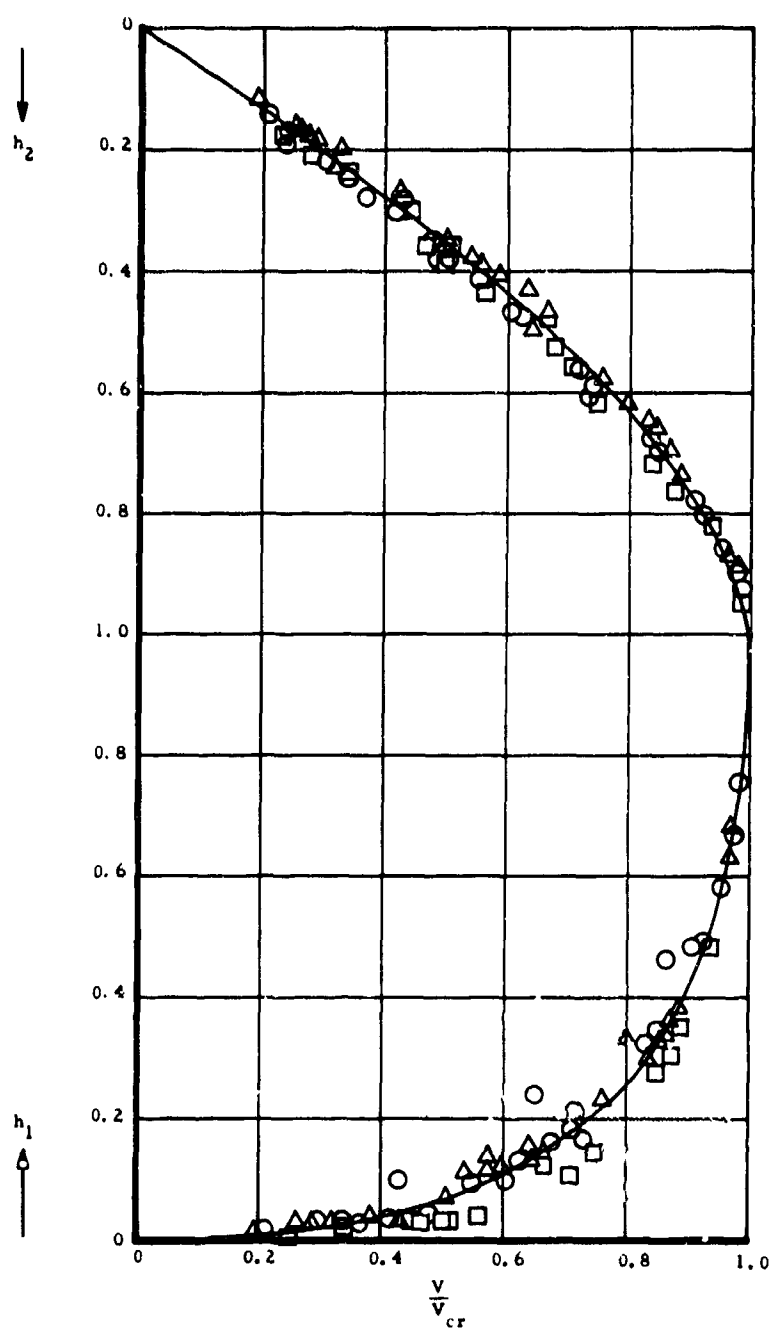
2. NON-DIMENSIONAL HEIGHT

a.-LOWER BOUNDARY OF H-V DIAGRAM  
FOR VELOCITY  $V_n$ , DETERMINE NON-  
DIMENSIONAL HEIGHT  $h_2$ , BY RATIO  
SHOWN IN FIGURE; WHERE  $h_2$  EQUALS  
HEIGHT OVER GROUND AT VELOCITY  
 $V_n$ ; AND  $h_{cr}$  AND  $h_{\min}$  ARE KNOWN  
VALUES AS DEFINED IN THE GLOSSARY

b.-UPPER BOUNDARY OF H-V DIAGRAM  
FOR SAME VELOCITY  $V_n$ , DETERMINE  
NON-DIMENSIONAL HEIGHT  $h_1$ , BY RATIO  
SHOWN IN FIGURE; WHERE  $h_1$  EQUALS  
HEIGHT OVER GROUND AT VELOCITY  
 $V_n$ ; AND  $h_{cr}$  AND  $h_{\max}$  ARE KNOWN  
VALUES AS DEFINED IN THE GLOSSARY

3. NON-DIMENSIONAL CURVE  
PLOT NON-DIMENSIONAL HEIGHTS AND  
VELOCITIES THUS OBTAINED AS SHOWN  
ON FIG. 4

FIG. 3 METHOD OF CONVERTING TYPICAL H-V DIAGRAM  
INTO CALCULATED KEY POINT RATIOS



MEAN CURVE VALUES		
$V/V_{cr}$	$h_1$	$h_2$
0	0	0
.10	0	.07
.20	.005	.13
.25	.01	.17
.30	.02	.20
.35	.025	.24
.40	.035	.28
.45	.05	.31
.50	.06	.35
.55	.08	.39
.60	.10	.43
.65	.13	.48
.70	.16	.53
.75	.20	.58
.80	.25	.63
.82	.27	.66
.84	.30	.68
.86	.33	.70
.88	.37	.73
.90	.40	.76
.92	.46	.79
.94	.52	.82
.96	.60	.85
.98	.68	.90
.99	.80	.93
1.00	1.00	1.00

FIG. 4 COMPOSITE NONDIMENSIONAL CURVE

Essentially,  $h_{min}$  and  $V_{cr}$  are the only unknowns. As will be shown later in this report,  $h_{cr}$  and  $h_{max}$  have been established by this program and  $h_{min}$  is empirically related to  $V_{cr}^2$ . It is necessary to test for only one of the two values (i.e.,  $h_{min}$  or  $V_{cr}$ ) to develop the H-V diagram. Since tests for  $h_{min}$  have been shown to be less accurate and more difficult to conduct than tests for  $V_{cr}$ , it would be more logical to test for  $V_{cr}$ .

### 3. Evaluation of Key Point Relationships

#### a. The Critical Speed Versus Weight

Each helicopter tested showed a linear relationship of  $V_{cr}$  versus weight over the range of weights and altitudes at which each were tested. Since only the helicopter utilized in Reference 1 was equipped with an altitude engine, it was the only helicopter which could be tested over a full weight range at the highest altitudes tested. There was no evidence of drag divergence or detrimental blade stall which would cause a serious alteration of the linear relation for an altitude range of at least sea level to 8000 feet. This was true for the one-second delay as well as the no-delay test results. In each of the three reports, an expression as shown below was presented from which  $V_{cr}$  for a new weight could be determined from a  $V_{cr}$  obtained at some test weight.

$$V_{cr} = V_{cr_{test}} + C_1 \Delta W \quad \text{where } C_1 = \frac{dV_{cr}}{dW}$$

Analysis of the three sets of test data revealed that if the experimentally determined values of  $C_1$  were multiplied by rotor area, the products were essentially constant; i.e.,

$$C_1 A = 22.6$$

The use of this empirically established relationship in the previous equation involving  $V_{cr}$ , results in an expression for the change in  $V_{cr}$  due to a weight change in terms of a delta disk loading; i.e.,

$$V_{cr} = V_{cr_{test}} + 22.6 \frac{\Delta W}{A}$$

so that a new  $V_{cr}$  can be readily obtained by applying an average value of  $C_1 A$  (22.6) to the delta disk loading.

Figure 5 was developed using the average test value of  $C_1 A = 22.6$ . From this chart  $C_1$  can be determined directly as a function of rotor disk area. Because of the representative, but widely varying basic parameters of the three helicopters tested, it is concluded that all conventional single-rotor helicopters will fit the experimentally determined value of 22.6 for  $C_1 A$ .

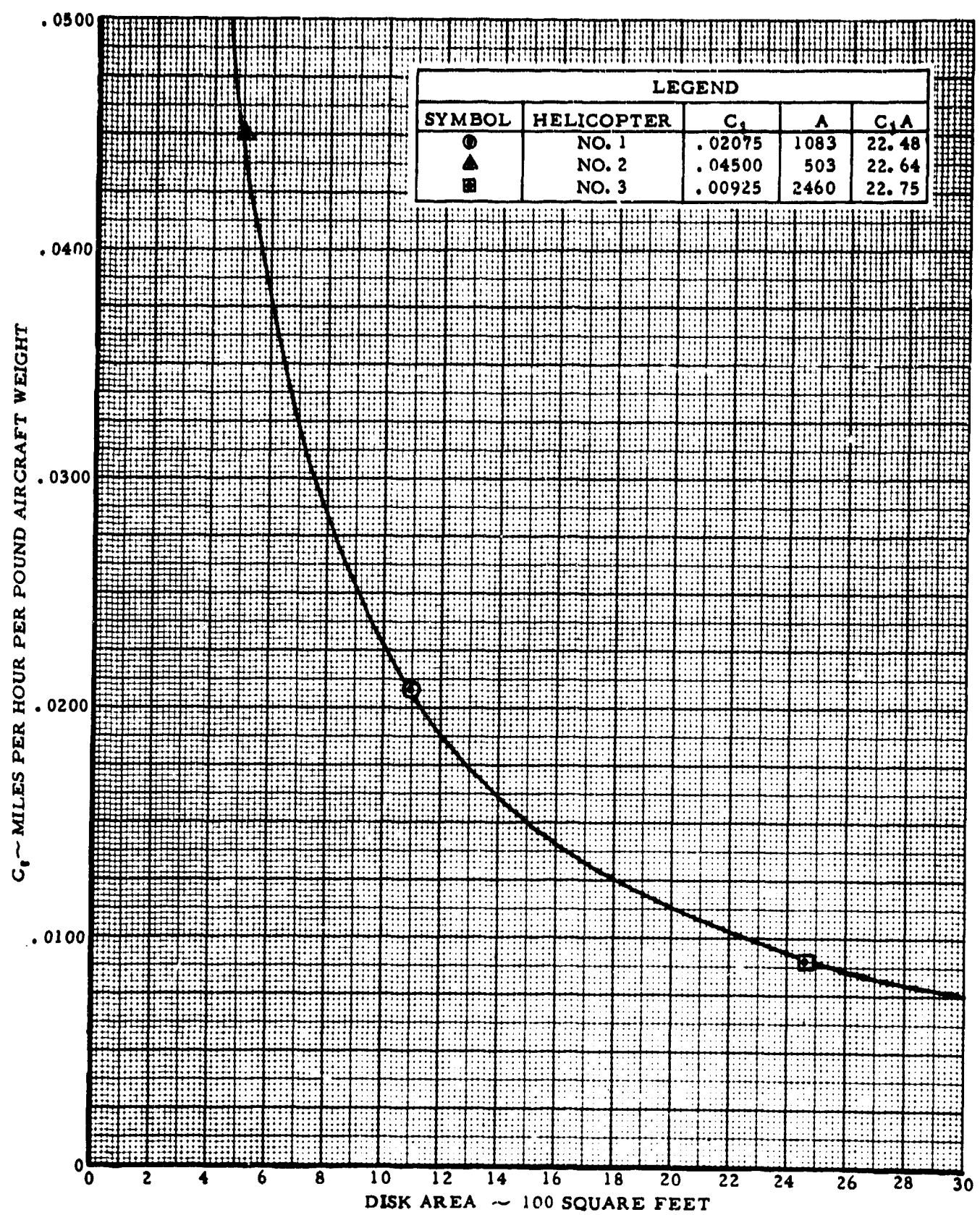


FIG. 5  $C_1$  VERSUS DISK AREA

b. The Critical Speed Versus Altitude

The basic purpose of this portion of the composite analysis was to establish the effects of altitude on the critical speed. The three project tests had proven rather conclusively that the variation of  $V_{cr}$  with altitude was linear and was valid over a normal altitude range of at least sea level to 8000 feet. The helicopters which were limited in power available could only be tested at lighter weights at the higher altitudes, but there was no evidence to suspect that for the normal altitude range there would be any deterioration from the linear characteristics. As in the case of  $V_{cr}$  versus weight, the linear relationship of  $V_{cr}$  versus altitude was maintained for both the no-delay and one-second delay test results. An increase in  $V_{cr}$  was experienced for a one-second delay and the increase was constant with altitude changes such that the linearity of  $V_{cr}$  versus altitude was not affected. No empirical solution was found for determining the change in  $V_{cr}$  due to a change in altitude on a unified basis involving all three helicopters as was done in the case of  $V_{cr}$  versus weight. In each of the three reports an expression as shown below was presented from which  $V_{cr}$  for a new altitude could be determined from a  $V_{cr}$  obtained at some other test altitude.

$$V_{cr} = V_{cr,test} + C_2 \Delta H_D \text{ where } C_2 = \frac{dV_{cr}}{dH_D}$$

The values of  $C_2$  obtained for each helicopter could not be correlated or combined with known parameters to arrive at a solution which was applicable to the three helicopters for the determination of  $V_{cr}$  at a different altitude, as was done in the case of  $V_{cr}$  versus weight. On a practical basis, however, the variation of  $C_2$  values determined for the three test aircraft are not so great as to preclude a working solution from the data obtained. The  $C_2$  values of the helicopters tested varies between 1.6 and 2.5 mph per thousand feet, with Helicopters Nos. 2 and 3 being 2.5 and 2.3 mph per thousand feet respectively. It should be pointed out that the helicopters tested encompassed an extreme range of the major parameters and therefore can be considered to encompass helicopters whose parameters fall within this range. It is not likely, therefore, that the value of  $C_2$  ( $dV_{cr}/dH$ ) for conventional single rotor helicopters will exceed the maximum value obtained in this program. Until such time as additional information is obtained to establish an empirical or theoretical relationship for  $C_2$ , the use of the maximum value of 2.5 mph per thousand and feet of altitude is a practical solution.

c. The Critical Height

The critical height,  $h_{cr}$ , was found to be reasonably constant over the altitude and weight range for all three helicopters and averaged approximately 100 feet. The critical height for Helicopter No. 1 (Reference 1) varied between 90 and 100 feet and was assumed to be constant at 95 feet. As a result of the tests of Reference 1, Helicopter

No. 2 was tested more critically in this area to determine if a variation existed in  $h_{cr}$ . This helicopter showed a variation in  $h_{cr}$  from 80 to 100 feet over the range of weights and altitudes tested. The diagrams of Helicopter No. 2 had originally been prepared with a pronounced "chin" or distention of the lower boundary. As a result of this analysis; i.e., analyzing the curves of all three helicopters collectively, it was determined that they could have been faired otherwise, which would result in not only reducing the chin but also in raising the critical height as well. Helicopter No. 3 showed a range of critical heights between 90 and 110 feet. Further analysis of all of the data indicated that at maximum gross weight at sea level,  $h_{cr}$  can be defined as approximately 100 feet. For lighter weights at sea level,  $h_{cr}$  would be somewhat lower and for higher altitudes at maximum gross weight,  $h_{cr}$  would be somewhat higher. Thus, with a weight reduction at altitude,  $h_{cr}$  would remain approximately constant at 100 feet. This finding was important to the determination of an H-V diagram because it permits the height at which  $V_{cr}$  occurs to be established.

d. Critical Speed Squared Versus High Hover Height

In each of the three previous reports a linear relation was found to exist between the high hover height,  $h_{min}$ , and the square of the critical speed,  $V_{cr}^2$ , as shown in Fig. 6. Since this appeared to be significant with respect to the H-V diagram, an analysis of this particular relationship was made for the three helicopters.

As there was a slight discrepancy between the  $h_{min}$  versus  $V_{cr}^2$  curves of the three helicopters, as shown in Fig. 6, the basic test data of all three were examined collectively. This examination led to the conclusion that one common curve could be drawn for all three helicopters. This was of particular significance since it appeared that the relationship of  $h_{min}$  and  $V_{cr}^2$  was the same for all helicopters independent of the helicopter parameters, and determination of one of these key points could be made if the other were known.

From this straight line common curve shown in Fig. 6, an empirical equation was established as follows:  $h_{min} = 200 + .1336 V_{cr}^2$ .

Conventional single rotor helicopters subscribe to this expression. This relationship, which associates the high hover point with the critical speed, made it possible to define the limits of the upper boundary of the H-V diagram by simply obtaining one of these points.

e. Low Hover Height Versus Weight and Altitude

The landing following power failure from the low hover height,  $h_{max}$ , is the one regime of flight on the H-V diagram which lends itself to an energy analysis and this has been effectively treated in Reference 5. A study was made of the low hover height and the lower boundary to obtain a simplified empirical solution. It was determined

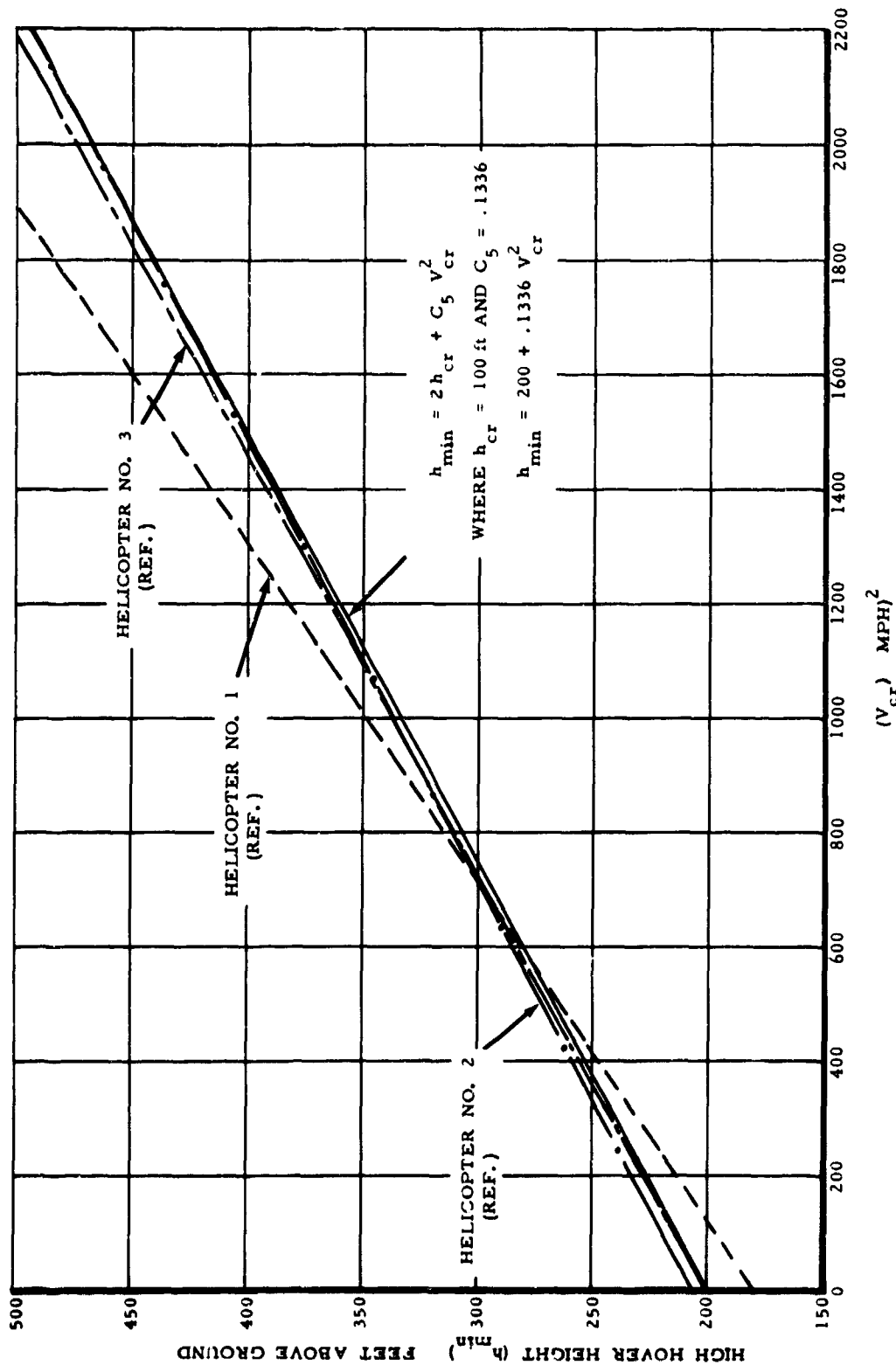


FIG. 6 HIGH HOVER HEIGHT ( $h_{min}$ ) VERSUS  
SQUARE OF CRITICAL VELOCITY ( $V_{cr}^2$ )

that the variation of  $h_{max}$  for any of the helicopters was small. Of the three helicopters tested, the largest variation encountered over the weight and altitude range was a variation in  $h_{max}$  from approximately 5 to 20 feet. The 10-foot height, generally accepted in lieu of conducting  $h_{max}$  tests, appears to be a realistic value for  $h_{max}$  at sea level and maximum gross weight. In the interest of conservatism, simplicity, and for purposes of maintaining the family relationship of H-V diagrams, it is recommended that a reduction of 1 foot of height in  $h_{max}$  per 1000 feet increase in density altitude be appropriately applied to the basic 10-foot sea level value. Similarly, for a weight reduction from maximum gross weight to minimum operating weight,  $h_{max}$  should be increased 5 feet above the basic 10-foot sea level value. The value of  $h_{max}$  thus derived provides the lower limit of the lower boundary portion of the H-V curve.

#### Factors Affecting the Autorotative Landing Following Power Failure

##### 1. Rotor Inertia and Rotor Speed

Two of the helicopters tested had a normal operating rotor speed which produced tip speeds of approximately 700 ft/sec. The lightweight helicopter rotor speed was on the low side with a tipspeed of 640 ft/sec. All three helicopters employed metal blades of the NACA 00 series and thus operated on approximately the same profile drag coefficient versus mean lift coefficient curve ( $C_D$  versus  $C_L$ ). The profile drag, therefore, was essentially the same since all three helicopters operated at approximately the same mean lift coefficient.

An investigation was made into the relative rotor speed decay to determine the effect of rotor inertia on rotor speed decay following throttle chop along the upper boundary. In order to compare the decay trends of the three helicopters, a plot of rotor speed in percent of rated rpm versus time was constructed as shown on Figure 7. It is interesting to note that the helicopter with the largest inertia per pound of aircraft weight (Helicopter No. 3) exhibits the largest percent decay with time. The data show that the decay rate relationship between the helicopters remains essentially the same whether a one-second delay or no-delay was employed following throttle chop prior to collective pitch reduction, although the percent decay is largest after a one-second delay. It should be noted also that following a one-second delay, the helicopter with the least inertia per pound of aircraft weight does not have the highest  $V_{cr}$  (sea level, maximum gross weight) and conversely, the helicopter with the most inertia per pound does not have the lowest  $V_{cr}$ . Thus it was not possible to establish any pattern of the effect of rotor inertia on  $V_{cr}$ , and other factors are obviously present in the development of  $V_{cr}$ .

Only a limited amount of testing was conducted in Reference 1 to determine the effects of added rotor inertia on the location of  $V_{cr}$  or the upper boundary of the H-V diagram. From this limited data the effects of inertia appeared minimal. Likewise, the test helicopters

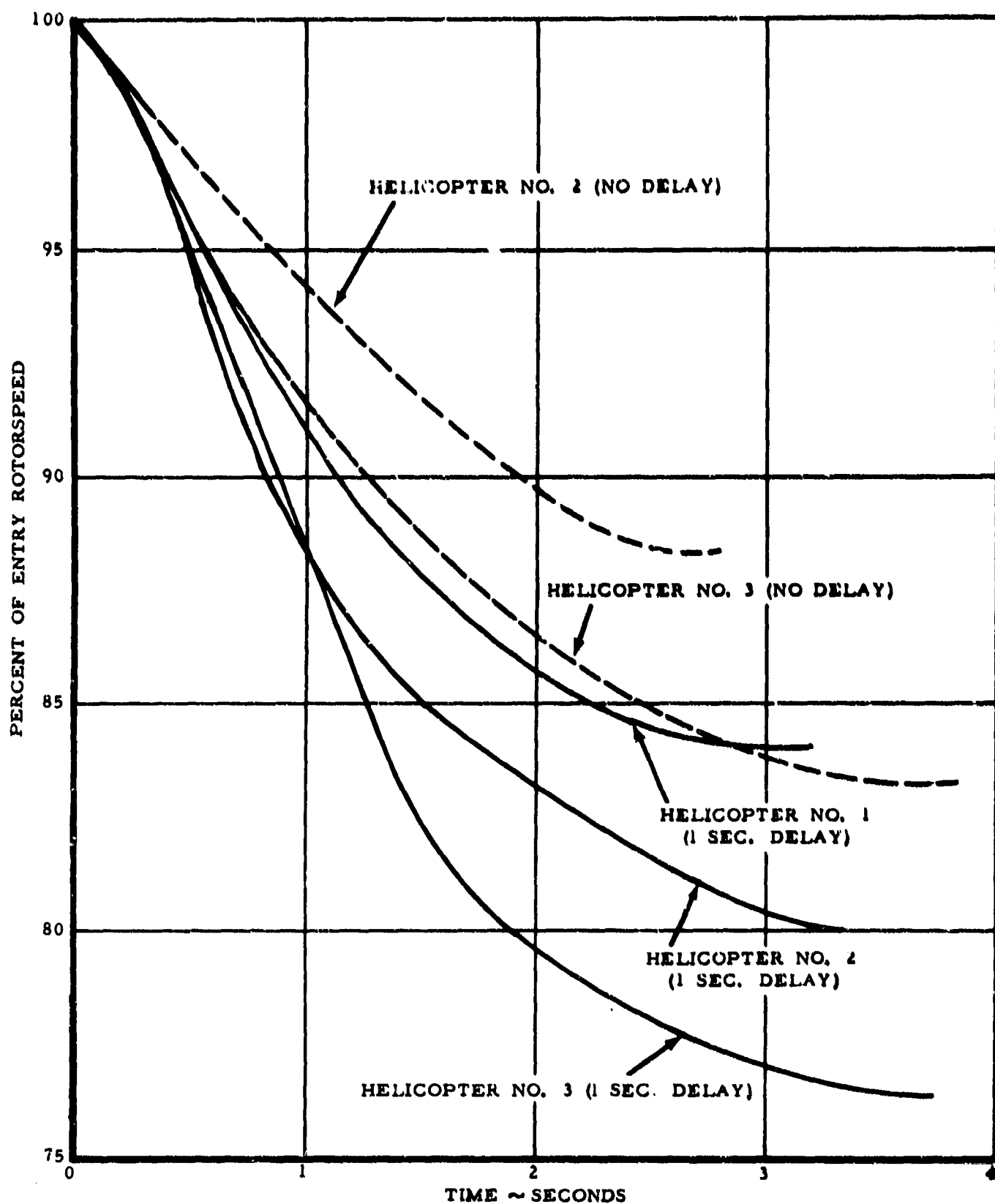


FIG. 7 AVERAGE ROTOR SPEED DECAY TRENDS  
FROM HIGH HOVER ENTRY POINTS

having varying inertia values per pound of aircraft weight from .1 to .6 displayed a consistent pattern in the  $h_{min} - V_{cr}$  relation and along the upper boundary. From high hover to  $V_{cr}$ , therefore, it is evident that there are factors other than rotor inertia which determine the values of  $h_{min}$  and  $V_{cr}$ .

### 2. Blade Stall Considerations

During the tests conducted on Helicopter No. 1, no comment was made by the pilot with respect to blade stall. There appeared to be no evidence of blade stall at any weight or altitude. The pilot never indicated that blade stall was a consideration. Blade stall did not become a consideration until the last test project. At the higher weights and generally throughout the altitude range during the tests of Reference 3, the pilot found it necessary to adjust his technique to compensate for the effects of blade stall during flare and final collective pull-up. There were occasions during the second helicopter test program when the pilot reported "falling through" the flare. Although he did not report it as blade stall, it is conceivable that blade stall was a factor in "falling through" the flare. It appears that blade stall as a factor in the autorotative landing following power failure is a function of disk loading. Helicopter No. 1, which had a relatively light disk loading, did not require high collective blade angles to effect its landings and this, undoubtedly, contributed to the lack of blade stall. On the other hand, Helicopter No. 3 with its extremely high disk loading needed all the blade angle possible which in turn contributed to blade stall as a factor. It is also possible that rotor inertia is an influencing factor in that the higher inertia rotor regains its rpm less rapidly in the flare, whereas, low inertia rotor regains its rpm more rapidly. Reference to Figure 7 shows that loss of rotor speed following throttle chop is a function of disk loading and not rotor inertia.

### 3. The Maneuver - Cyclic and Collective Flare

Analysis of the time histories of all three helicopters showed that the cyclic and collective controls were utilized in similar fashion and produced traces of pitch attitude, acceleration, swashplate angle, and blade angle which were repetitive in pattern. This can be seen in Figures 8 through 10, which show sample time histories of the three aircraft for the three basic H-V diagram areas - high hover, low hover, and  $V_{cr}$ . The deceleration following power failure along the upper boundary from  $h_{min}$  to  $V_{cr}$ , for example, consistently showed approximately .75g from 1g steady level flight. There was clear evidence in the time histories that when power failure occurred along the upper boundary, the cyclic flare was the most important control factor in executing a power-off landing. While the collective pitch was vital to reducing the load

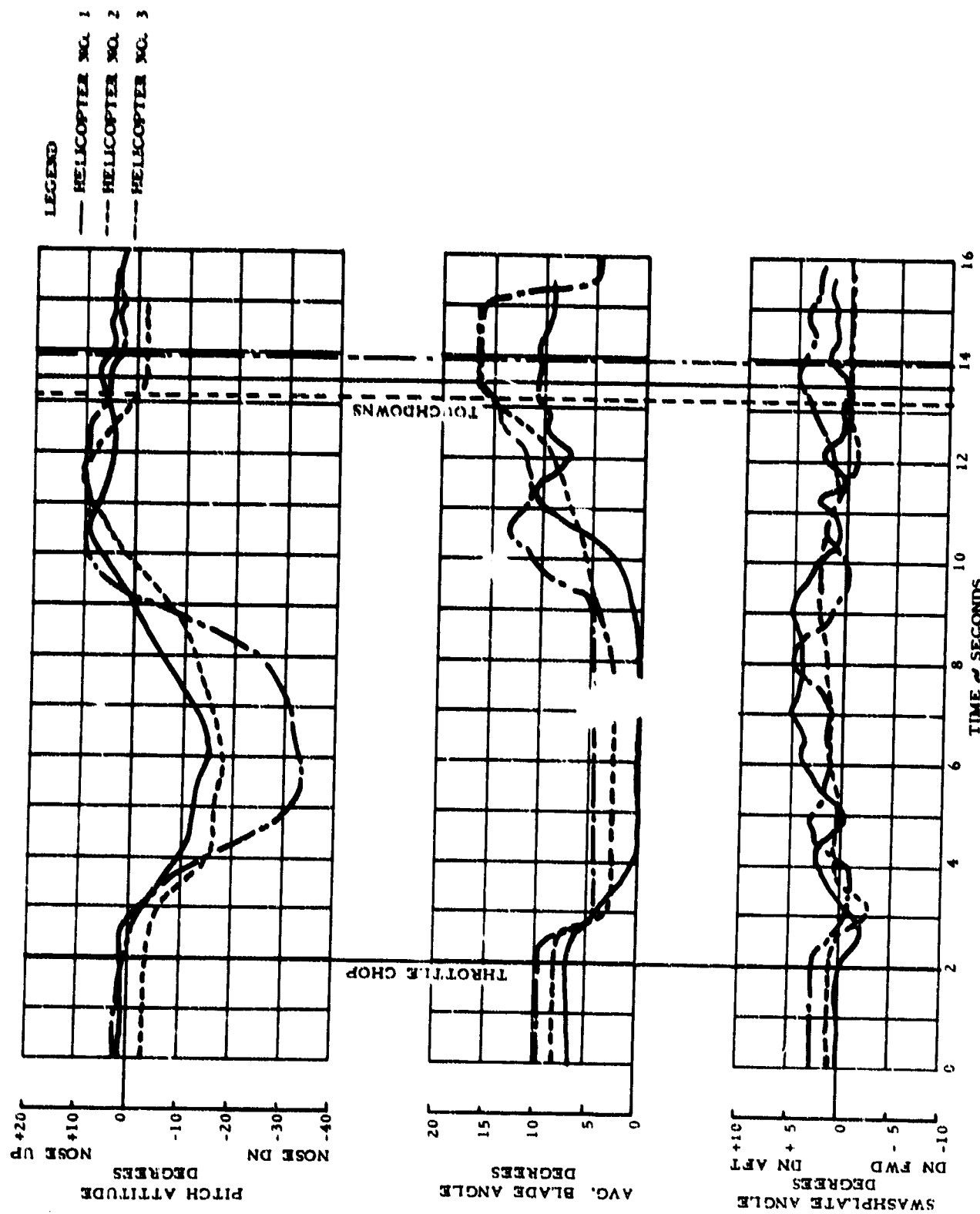


**FIG. 8 COMPARISON OF TIME HISTORY DATA FOR HIGH HOVER POINTS - THREE TEST HELICOPTERS**

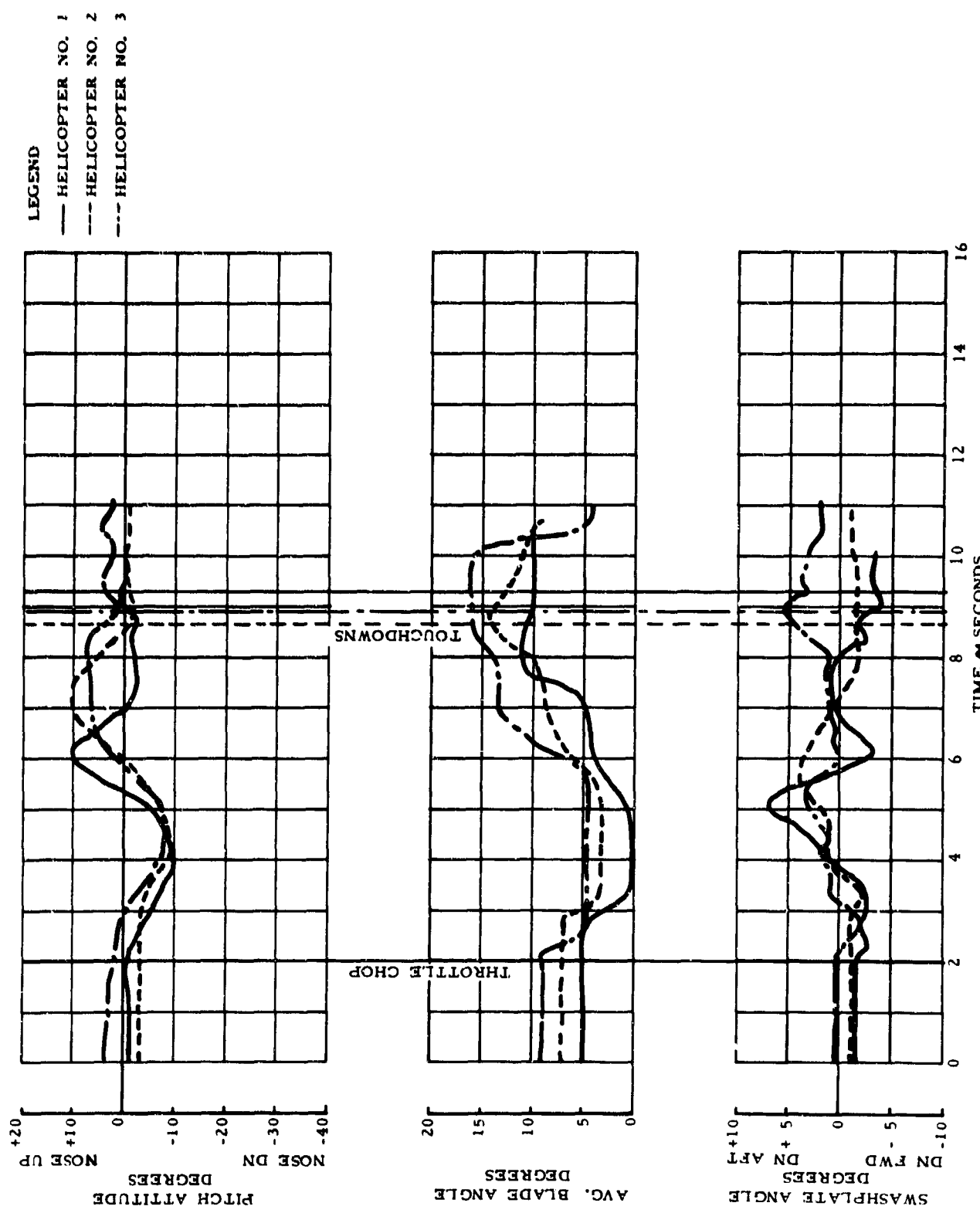
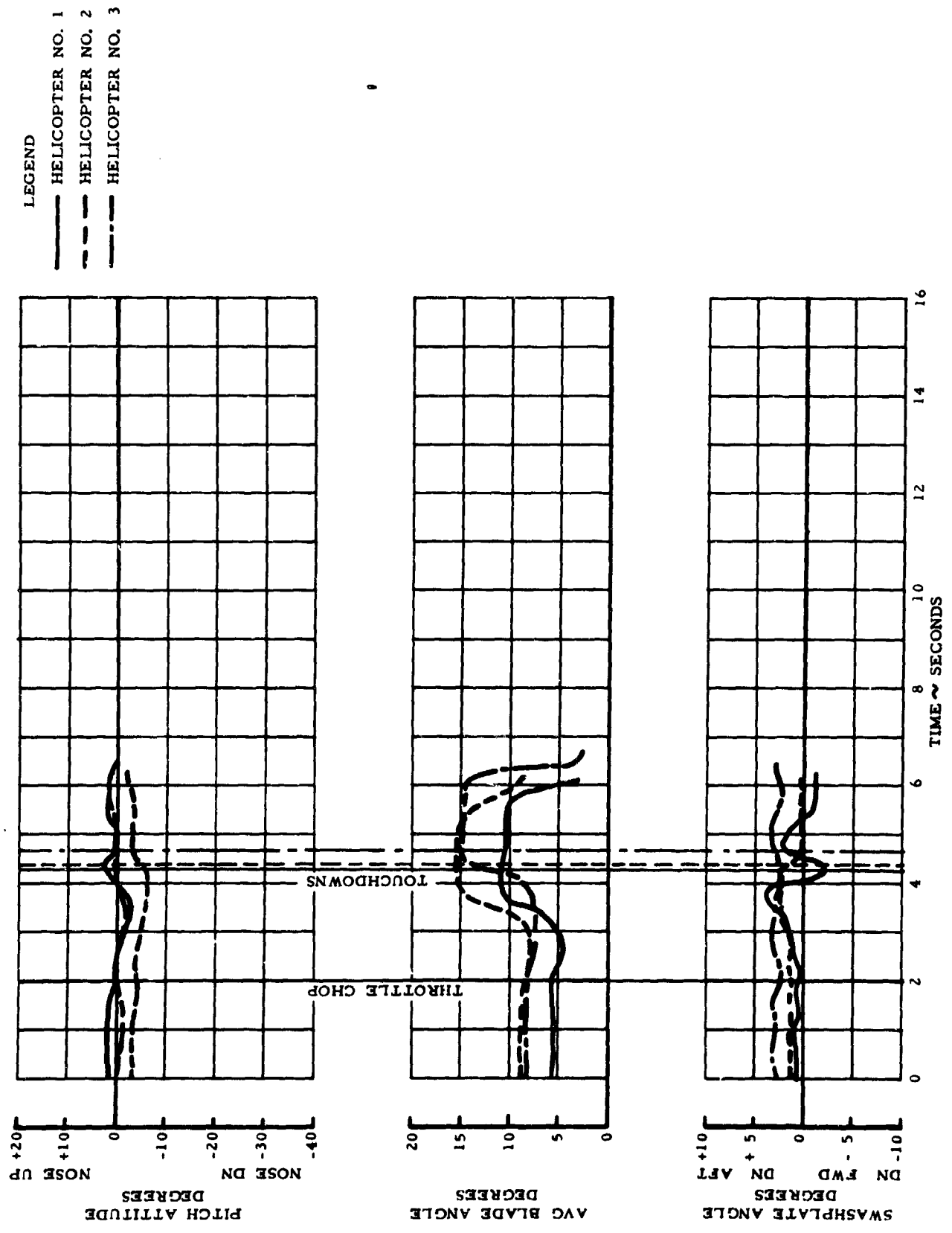


FIG. 9 COMPARISON OF TIME HISTORY DATA FOR CRITICAL SPEED AREA ( $V_{cr}$ ,  $h_{cr}$ ) - THREE TEST HELICOPTERS



**FIG. 10 COMPARISON OF TIME HISTORY DATA FOR LOW HOVER POINTS - THREE TEST HELICOPTERS**

factor on contact, it was the cyclic flare that generated the rotor speed and rate of descent reduction which made a good collective flare possible. Without this technique, significantly greater air-speed was required prior to contact for a good collective flare.

The landing techniques employed for the three helicopters were reasonably consistent, even though Helicopters Nos. 1 and 2 had skid gears and Helicopter No. 3 had a tail wheel/mainwheel configuration. In the case of Helicopter No. 3, the technique was basically the same as that employed for the skid gear helicopters even though the technique did not call for leveling the helicopter before contact. In landing Helicopter No. 3 it was necessary to apply only partial collective pitch to cushion the tailwheel while "feeling for the ground." The remaining collective application was applied to cushion the main gear touchdown which determined the acceptable load factors. The helicopter was landed, therefore, with a technique midway between an air rotation for level landing (as were the skid gear aircraft) and a pure flare landing (as would be done for a main wheel aft configuration).

Referring again to Figures 8 through 10, it can be seen that all the essential elements of control and aircraft motion are similar for the three aircraft. During the tests and subsequent data analysis of Helicopter No. 2, it was believed that distortion of the lower boundary occurred because of the low rotor inertia. There was insufficient time from throttle chop to touchdown to regain rotorspeed through a cyclic flare, and therefore, the landings had to be made essentially by means of a collective flare. Subsequent testing on Helicopter No. 3, however, showed that the same condition existed on the high inertia rotor. Points developed along the lower boundary with Helicopter No. 3 were also accomplished with minimum cyclic flare and maximum collective flare. The time from throttle chop to touchdown was insufficient for the high inertia rotor to build back any rotor speed, so that essentially, the techniques employed were consistent for all helicopters. It is the time element between throttle chop and touchdown, established by the entry altitude and speed, which dictates the type of maneuver necessary along the lower boundary. Rotor inertia appeared to have a very small influence on this regime of flight.

#### Method for Converting Test Program H-V Diagrams to Flight Manual Type H-V Diagrams

The results of the tests conducted in this program established that along the upper boundary the use of a one-second delay simply added an increment of speed such that the upper boundary was displaced laterally. The one-second delay diagrams complied with the patterns established in the Height Velocity Diagram section of this report and were, therefore, subject to the nondimensionalized form. Since the upper boundary of the flight manual type H-V Diagram is determined utilizing

a one-second delay, it is apparent that the curves should be identical except for a margin of conservatism to differentiate between the maximum performance data obtained by professional pilots in this program and the capabilities of the average pilot. If an appropriate margin is thus applied to  $V_{cr}$ , a flight manual type H-V diagram upper boundary can be developed by a single point determination of a maximum performance  $V_{cr}$  at an  $h_{cr}$  of 100 feet. Furthermore, since we have nondimensionalized the H-V diagram, the lower boundary when developed from the same  $V_{cr}$  will provide a lower boundary that will be equivalent to the accelerated climbout technique generally utilized in establishing the lower boundary. In this regime a one-second delay is not employed; therefore, the two increments in  $V_{cr}$  from no-delay to one-second delay, and from one-second to the percent margin increase, provides the necessary margin for the accelerated climbout lower boundary.

Procedures for Obtaining Flight Manual Type H-V Diagrams for Range of Weights and Altitudes

A procedure for developing a flight manual type H-V diagram established in accordance with the data and determinations contained in this report would make it possible to obtain a set of H-V diagrams over a range of weights and altitudes from a single test to determine  $V_{cr}$ . The following procedure, therefore, is considered reasonable for establishing such a flight manual type H-V diagram.

1. At a given gross weight (near maximum), and at a given density altitude (near sea level), and with a neutral c.g., determine a maximum performance  $V_{cr}$  with a one-second delay at an  $h_{cr}$  of 100 feet.

2. Using Figure 5, determine  $C_1$  and use the equation  $V_{cr} = V_{cr,test} + C_1 \Delta W$  to establish  $V_{cr}$  for maximum gross weight. Likewise, using the value of  $C_2$  of 2.5 mph per 1000 feet, correct  $V_{cr}$  for sea level using the equation  $V_{cr} = V_{cr,test} + C_2 \Delta H_D$ . A  $V_{cr}$  for maximum gross weight at sea level has now been established.

3. Add to the  $V_{cr}$  established in Item 2, above, an increment of speed (in mph) to provide an adequate safety margin for the average pilot.

4. Using the equation  $h_{min} = 200 + .1336 V_{cr}^2$ , determine  $h_{min}$ . Select an  $h_{max}$  of 10 feet an  $h_{cr}$  of 100 feet.

5. With  $V_{cr}$ ,  $h_{cr}$ ,  $h_{min}$ , and  $h_{max}$  now known, establish the H-V diagram using the nondimensional data from the mean curve chart of Figure 4 and the equations for  $h_1$ ,  $h_2$ , and  $V_n/V_{cr}$  shown on Figure 3. A flight manual type H-V diagram for maximum gross weight at sea level has now been established.

6. Using  $C_1$  and  $C_2$  establish  $V_{cr}$  for all desired weights and altitudes.

7. Determine  $h_{min}$  as in Step 4. for each  $V_{cr}$ .

8. Determine  $h_{max}$  by subtracting 1 foot per 1000 feet of density altitude from the basic 10 feet for sea level maximum weight and adding 5 feet over the weight range from maximum weight to minimum operating weight.

9. Determine  $h_{cr}$  by adding 1 foot per 1000 feet of altitude to the basic 100 feet at constant weight and decrease 10 feet equally spaced over the operating weight range for constant altitude.

10. Knowing all key points, repeat as in Step 5. and obtain a family of H-V diagrams over the desired weight and altitude range.

11. Spot check the diagrams with average pilot technique at critical c.g.

12. Establish a procedure for utilizing the diagrams thus developed that is appropriate to the particular helicopter in accordance with its operating weight range and its hovering performance capabilities.

## CONCLUSIONS

Based upon an analysis of the data obtained in this program and an analytical study of the results in terms of basic helicopter parameters, it can be concluded that

1. A practical method has been evolved for determining a family of flight manual type H-V diagrams for any single engine, single rotor helicopter over a range of weights from maximum to minimum operating, and altitudes from sea level to 8000 feet, by utilizing a single maximum-performance test point determination of  $V_{cr}$ .

2. The H-V diagrams of any single rotor helicopter form a family of curves which are defined by a set of linear equations involving the key points of the H-V diagram,  $V_{cr}$ ,  $h_{cr}$ ,  $h_{min}$ ,  $h_{max}$ , which vary as follows:

a. The variation of  $V_{cr}$  with a change in weight is a function of disk loading and gross weight.

b. The variation of  $V_{cr}$  with a change in altitude can be accepted for practical purposes as varying 2.5 mph per 1000 foot change of density altitude.

c. The critical height ( $h_{cr}$ ) is approximately 100 feet at sea level and maximum gross weight increasing 1 foot per 1000 feet of density altitude and decreasing 10 feet over the weight range from maximum weight to minimum operating weight.

d. The high hover height ( $h_{min}$ ) varies linearly as the square of the critical speed and can be expressed in equation form as -

$$h_{min} = 200 + .1336 V_{cr}^2$$

where  $V_{cr}$  is in mph

$h_{min}$  is in ft

e. The low hover height ( $h_{max}$ ) is approximately 10 feet at sea level and maximum gross weight decreasing 1 foot per 1000 feet of density altitude and increasing 5 feet over the operating weight range from maximum weight to minimum operating weight.

3. Height-velocity diagrams can be generalized in nondimensional terms.

## RECOMMENDATIONS

Based upon the results of this summary analysis, it is recommended

1. In the interest of standardization, reduction of flight test risks through better predictions, and a reduction of testing at several altitudes, that consideration be given to using  $V_{cr}$  procedures and criteria of this report as guidance material in developing flight manual type H-V diagrams required in the fulfillment of the airworthiness standards for normal category rotorcraft (FAR 27.79).
2. Further study and flight testing be initiated to determine the relationship of  $V_{cr}$  with the basic helicopter parameters which may provide a means of H-V diagram determination without the requirement for any flight testing.

#### REFERENCES

1. Hanley, W. J., and Devore, G., An Evaluation of the Effects of Altitude on the Height Velocity Diagram of a Single Engine Helicopter, Technical Report ADS-1, February 1964.
2. Hanley, W. J., and DeVore, G., An Evaluation of the Effects of Altitude on the Height Velocity Diagram of a Lightweight, Low Rotor Inertia, Single Engine Helicopter, Technical Report ADS-46, July 1965.
3. Hanley, W. J., Devore, G., and Martin, S., An Evaluation of the Height Velocity Diagram of a Heavyweight, High Rotor Inertia, Single Engine Helicopter, Technical Report ADS-84, November 1966.
4. Rich, M. J., An Energy Absorption Safety Alighting Gear for Helicopter and VTOL Aircraft, IAS Paper No. 62-16, January 1962.
5. Pegg, R., Calculating Changes in the Helicopter Height Velocity Diagram with Changes in Density Altitude and Gross Weight, University of Virginia Master's Thesis, May 1965.

**APPENDIX 1**  
**GLOSSARY OF TERMS**

## GLOSSARY OF TERMS

<u>H-V Diagram</u>	A graphical presentation which defines an envelope of flight with respect to airspeed and height above the ground, within which, in the event of power failure, a safe power-off landing could not be accomplished.
<u>Key Points</u>	The critical points on the H-V diagram which define the size of the diagram. They are $h_{min}$ , $h_{max}$ , and $V_{cr}$ , $h_{cr}$ as defined below.
<u>Upper Boundary</u>	The curve describing that portion of the H-V diagram between the high hover point ( $h_{max}$ ) and the point for critical speed ( $V_{cr}$ , $h_{cr}$ ).
<u>Lower Boundary</u>	The curve describing that portion of the H-V diagram between the low hover point ( $h_{min}$ ) and the point for critical speed ( $V_{cr}$ , $h_{cr}$ ).
<u>"Knee"</u>	A colloquial term that is synonymous with that curved portion of the H-V diagram in close proximity of the point for critical speed ( $V_{cr}$ , $h_{cr}$ ).
<u>Conventional Single Rotor Helicopter</u>	A helicopter which employs a gear and/or belt system for transmitting power to the main rotor, and does not utilize main rotor tip drive of any kind.
<u><math>V_{cr}</math></u>	Critical Velocity. The speed above which an autorotative landing can be made from any height after power failure in the low speed regime, mph, CAS.
<u><math>h_{cr}</math></u>	The height above the ground at which $V_{cr}$ occurs, ft.
<u><math>h_{min}</math></u>	The high hover height - the height above the ground from above which a safe autorotative landing can be made after power failure at zero airspeed, ft.
<u><math>h_{max}</math></u>	The low hover height - the height above the ground from below which a safe power off landing can be made after power failure at zero airspeed, ft.
<u><math>H_p</math></u>	Density altitude at the point of landing, ft.
<u><math>h</math></u>	Height of the helicopter above the ground, ft.
<u><math>W</math></u>	Helicopter weight, lb.

## GLOSSARY OF TERMS CONTINUED

- C<sub>A</sub>: Calibrated airspeed = indicated airspeed corrected for instrument and position error, mph.
- C<sub>1</sub>: The slope of the linear relationship of the change in critical speed with change in weight =  $\frac{dV_{cr}}{dW_D}$
- C<sub>2</sub>: The slope of the linear relationship of the change of the high hover height ( $h_{n1}$ ) with change in the square of the critical speed ( $V_{cr}^2$ ) =  $\frac{d h_{n1}}{dV_{cr}^2}$ .
- J: Equivalent flat plate area = ft<sup>2</sup>.
- A: Main rotor area = ft<sup>2</sup>.
- I<sub>D</sub>: Inertia of the dynamic system = slug ft<sup>2</sup>.
- V<sub>n1</sub>: Any arbitrarily selected velocity between zero and the value of the critical velocity ( $V_{cr}$ ) (used with Fig. 3 only)
- h<sub>n1</sub>: The height above the ground on the H-V diagram lower boundary that corresponds with the value of  $V_n$  (used with Fig. 3 only)
- h<sub>n2</sub>: The height above the ground on the H-V diagram upper boundary that corresponds with the value of  $V_n$  (used with Fig. 3 only)